Hindawi
Wireless Communications and Mobile Computing
Volume 2019, Article ID 8986302, 10 pages
https://doi.org/10.1155/2019/8986302

Research Article

A Self-Powered PMFC-Based Wireless Sensor Node for Smart City Applications

Daniel Ayala-Ruiz,[1] Alejandro Castillo Atoche,[2] Erica Ruiz-Ibarra,[1] Edith Osorio de la Rosa,[3] and Javier Vázquez Castillo[4]

[1]*Department of Electronics Engineering, Technology Institute of Sonora, Ciudad Obregon Sonora, Mexico*
[2]*Embedded System Department, Autonomous University of Yucatan, Merida Yucatan, Mexico*
[3]*Catedras CONACYT and Division of Sciences and Engineering, University of Quintana Roo, Chetumal Quintana Roo, Mexico*
[4]*Division of Sciences and Engineering, University of Quintana Roo, Chetumal Quintana Roo, Mexico*

Correspondence should be addressed to Javier Vázquez Castillo; jvazquez@uqroo.edu.mx

Received 23 March 2019; Revised 2 May 2019; Accepted 19 May 2019; Published 3 June 2019

Guest Editor: Zoran Stamenkovic

Long power wide area networks (LPWAN) systems play an important role in monitoring environmental conditions for smart cities applications. With the development of Internet of Things (IoT), wireless sensor networks (WSN), and energy harvesting devices, ultra-low power sensor nodes (SNs) are able to collect and monitor the information for environmental protection, urban planning, and risk prevention. This paper presents a WSN of self-powered IoT SNs energetically autonomous using Plant Microbial Fuel Cells (PMFCs). An energy harvesting device has been adapted with the PMFC to enable a batteryless operation of the SN providing power supply to the sensor network. The low-power communication feature of the SN network is used to monitor the environmental data with a dynamic power management strategy successfully designed for the PMFC-based LoRa sensor node. Environmental data of ozone (O_3) and carbon dioxide (CO_2) are monitored in real time through a web application providing IoT cloud services with security and privacy protocols.

1. Introduction

The concept of smart cities and Urban Internet of Things (IoT) is an important research field with the aim to make a better use of the public resources and increase the quality of the services offered to the citizens, while operational costs of the public administration are reduced [1]. In this scenario, the interconnection of sensor nodes (SNs) within a wireless sensor network (WSN) can be used to monitor environmental parameters. At the same time, the integration of an IoT-WSN enables the interconnection of the SNs with the Internet, opening a wide opportunity of end-user applications and Web services. Even though the technology advances in embedded systems with many low-power sensors, microcontroller, and transceivers for digital communications, there is still a great challenge in the power supply of these SNs. In general, these devices are usually powered by batteries; this constrains the lifetime of the network since they need to be replaced or recharged after a certain period of time.

Currently, several approaches have been developed to prolong the lifetime of SNs, e.g., covering routing protocols, sensing techniques, low-power WSN standards, among others [2–5]. Energy harvesting (EH) is one of the most promising techniques for this purpose, allowing SNs to operate autonomously by collecting and storing energy from the environment. Energy harvesting systems are typically composed of three components: energy source, energy harvesting module, and load (e.g., microcontroller, sensors, wireless transceivers, among others). In this sense, energy plays a leading role in smart cities as in most of our everyday activities, where an advantage of natural resources can be taken. These energy sources can be typically classified as mechanical, radiant, thermal, fluid flow, electromagnetic, and hybrid [5–9]. In this regard, new types of energy sources

have emerged and are still under development, such as the case of Plant Microbial Fuel Cells (PMFCs). PMFC is a green technology that generates energy through an electrochemical process based on the degradation of plant roots via active bacteria [10–12]. A PMFC is able to provide a continuous time-variant power that is managed by the energy harvesting module and stored in a supercapacitor, which can handle a large number of recharge cycles with a high charge-discharge efficiency, and without the need of a complex charge circuitry, albeit at the cost of higher self-discharge rate and lower weight-to-energy density compared with batteries [5, 6].

In this context, a WSN with PMFC-EH is suitable for smart cities, where real-time data acquisition is required in order to improve the collection, aggregation, and use of data using low-cost sensors and low-power communication systems. Authors in [13] designed a self-powered wearable IoT sensor network to monitor environmental conditions. The system incorporates a solar cell, supercapacitors as a storage device, and a LoRa-based wireless transmission module. Even though photovoltaic cells are powerful devices, they provide intermittent energy and depend on environmental conditions (i.e., sun light). Pietrelli et al. [12] reported a Terrestrian Microbial Fuel Cell (TMFC) able to produce a maximum power of 310 μW on a soil characterized by a pH of 7.6 and a controlled temperature. The TMFC provided energy to a WSN where IEEE 802.15.4 (Zigbee protocol) based transceivers were tested transmitting a single bit. The experiments showed that is possible to power a sensor node with a TMFC; however, a more realistic load needs to be tested. This is because the energy consumption of the sensor and microcontroller are not considered in the experiments which would result in a transmission cost increase. Finally, authors in [14] reported a PMFC-EH system for an IoT-based WSN based on Cordyline fruticosa plant. The designed PMFC was able to provide 3.5 mW/cm^2 with 0.7 V and 5 mA. The sensor node senses temperature and humidity with a dynamic power management strategy, and data is transmitted using Zigbee. However, several new wireless technologies (e.g., LoRa, Sigfox, and NB-IoT) promise better performance than Zigbee for applications where low-power and long-range are required [15].

The objective of this paper is to propose an IoT-based sensor network design with self-powered PMFC-EH architecture aiming to prolong the lifetime of the network for continuous environmental analysis. The PMFC, based on a Sansevieria asparagaceae plant, is able to produce a stable output voltage, allowing the energy harvesting circuit to harvest energy from the PMFC enabling a continuous DC energy supply for the SN. The mean power consumption of the SN is approximately 2.92 mW, considering the sensor measurements, microcontroller processing tasks, and wireless transmission. In addition, experimental results demonstrate a batteryless operation of the PMFC-based LoRa sensor network for environmental monitoring of smart cities.

The rest of the paper is organized as follows: Section 2 describes the PMFC, energy harvesting circuit, and sensor node data acquisition. In Section 3, the performance analysis of the self-powered PMFC-based LoRa sensor network is showed and discussed. Finally, Section 4 presents the conclusions.

2. IoT-Energy Harvesting System Design

The sensor node energy consumption must be adequate to accomplish an autonomous operation of the IoT WSN; this includes the SN processing tasks and LoRa wireless transmission. The energy harvesting circuit is adapted to PMFC as a power supply, providing a regulated voltage to the microcontroller, ozone (O_3) and carbon dioxide (CO_2) sensors, and LoRa-based transceiver. Figure 1 shows the conceptual architecture of a PMFC-EH system for the proposed sensor node. The following subsections describe the components of the system architecture.

2.1. Plant Microbial Fuel Cell (PMFC). PMFC is a power source that generates energy through the anaerobic degradation of organic matter via rhizosphere bacteria in a sustainable way, having a potential application in supplying electricity to devices. The use of PMFCs can be found in applications for monitoring environmental parameters, maturity of plants, bioremediation, and heavy metal recovering of contaminated environments [10, 11, 16–18].

According to the plant classification in [19], C3 and C4 type of plants achieve a high photosynthetic efficiency by converting the carbon dioxide (CO_2) into a four-carbon sugar compound [20]. Also, these types of plant have a high-rate of solar energy conversion into electrical energy with an increase of rhizosphere surface area for microbiome proliferation. Most microorganisms tend to transfer electrons produced from the metabolism of organic debris. On one hand, the plant root zone provides substrate in the form of root exudates to microbes, and on the other hand, microbes simplify the elemental form of nutrients to an ionic form amenable to the plant [21].

The electrodes are usually separated by a proton exchange membrane, which can be of Na ion [22] or a salt bridge [23]. However, membrane-less PMFC configurations have been reported, where the PMFC-cathode is placed in an oxygen-rich environment [24, 25]. Thus, the PMFC electricity is driven by rhizodeposition of the living plants [19].

The rhizodeposition contains a wide variety of carbon sources that can be used as electrodes, which represent a unique feature of PMFCs. In PMFC designs, the distance between anode and cathode, the dimensions of the electrodes, and the type of plant should be considered as shown in Figure 2.

As illustrated in Figure 2, the plant was placed above the anode and the separation between anode and cathode is 5 cm. The substrate availability per square meter can be improved by increasing the distance among the anode and the plant. Thus, the more roots are between the anode and plant, and the higher rhizodeposition would result. Moreover, studies report that increasing the depth of the anode with a factor of 3 results in more substrate, and consequently, a higher current density and output power can be harvested [23].

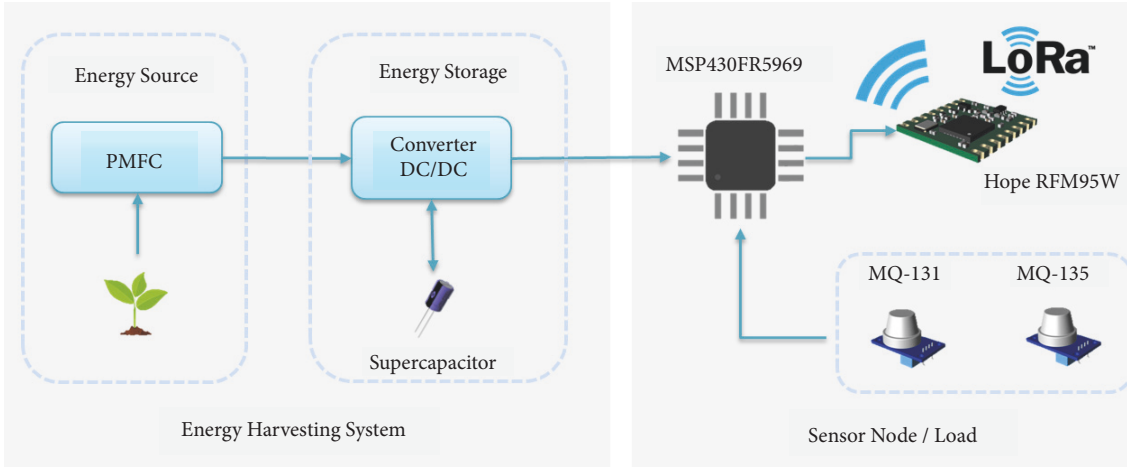

Figure 1: Conceptual self-powered sensor node architecture.

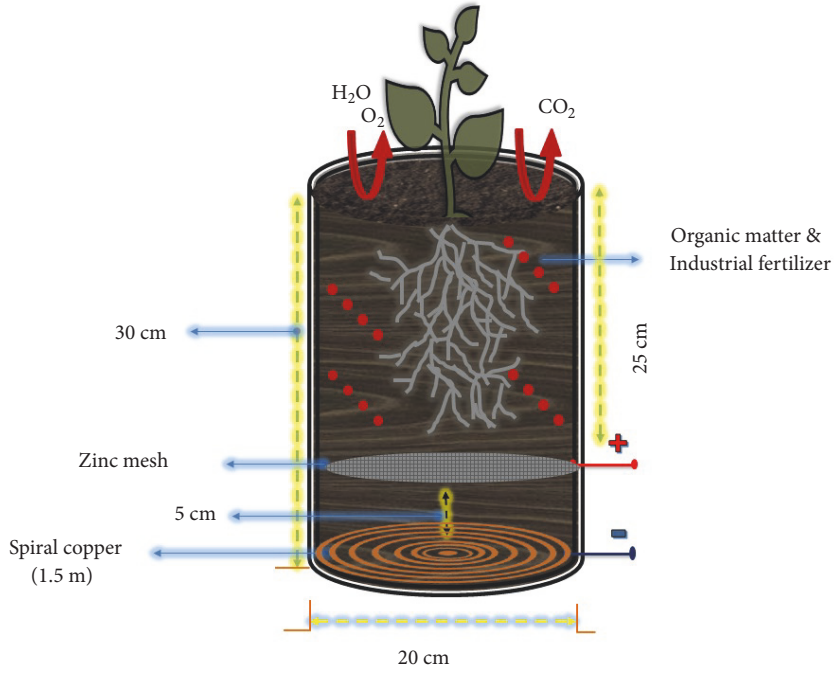

Figure 2: Schematic design of the PMFC used as IoT WSN power source.

2.2. Energy Harvesting Circuit. In order to extract the maximum power from the proposed PMFC, it is necessary to use an energy harvesting circuit with the aim of storing power in an external device such as supercapacitors. However, this kind of power sources (e.g., photovoltaic, piezoelectric, among others) is prone to voltage variations due to physical environmental changes, which results in dynamic power charges. Thus, it is necessary to use an efficient energy harvester management module.

The BQ25570 is a nano-power boost charger and buck converter for energy harvester powered applications that manages energy from an input voltage as low as 100 mV, which allows to use this device in thermoelectric generators, small solar cells, piezoelectric generators, among others. Also, this device was specifically designed to efficiently acquire and manage microwatts (μW) to milliwatts (mW) of power generated from a variety of high output impedances.

The used energy harvester management module can be observed in Figure 3. For our application, the voltage provided by the PMFC is enough to guaranty the BQ25570 operation. The boost converter is powered from output V_{Stor}. Once the V_{Stor} voltage is above V_{Stor_Chgen} (1.8 V typically), the boost converter can effectively extract power from the PMFC. The V_{Out} voltage is externally programmed to slightly less than the V_{Stor} voltage [26]. Likewise, it implements a programmable maximum power point tracking (MPPT)

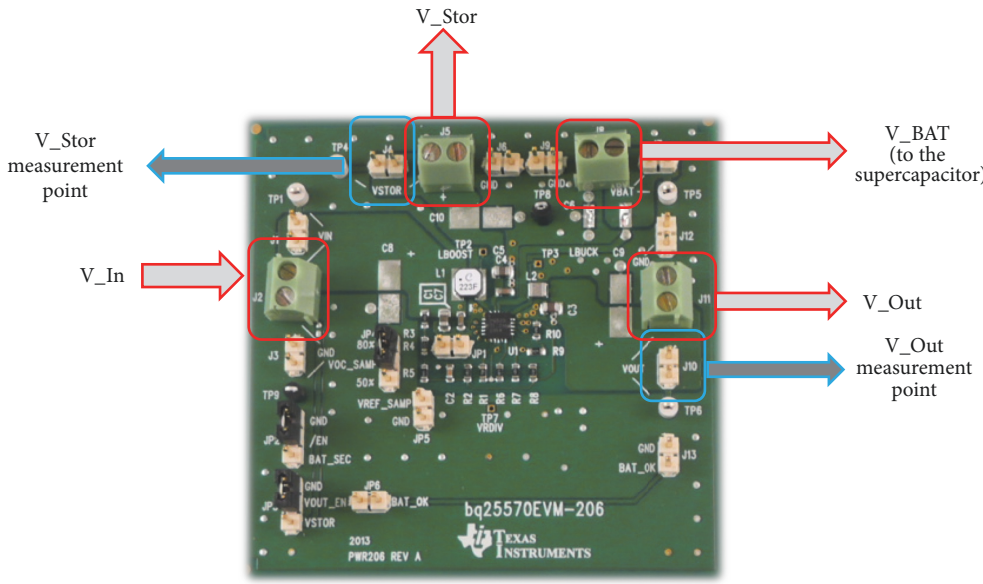

Figure 3: Energy harvester subsystem based on BQ25570 power management module.

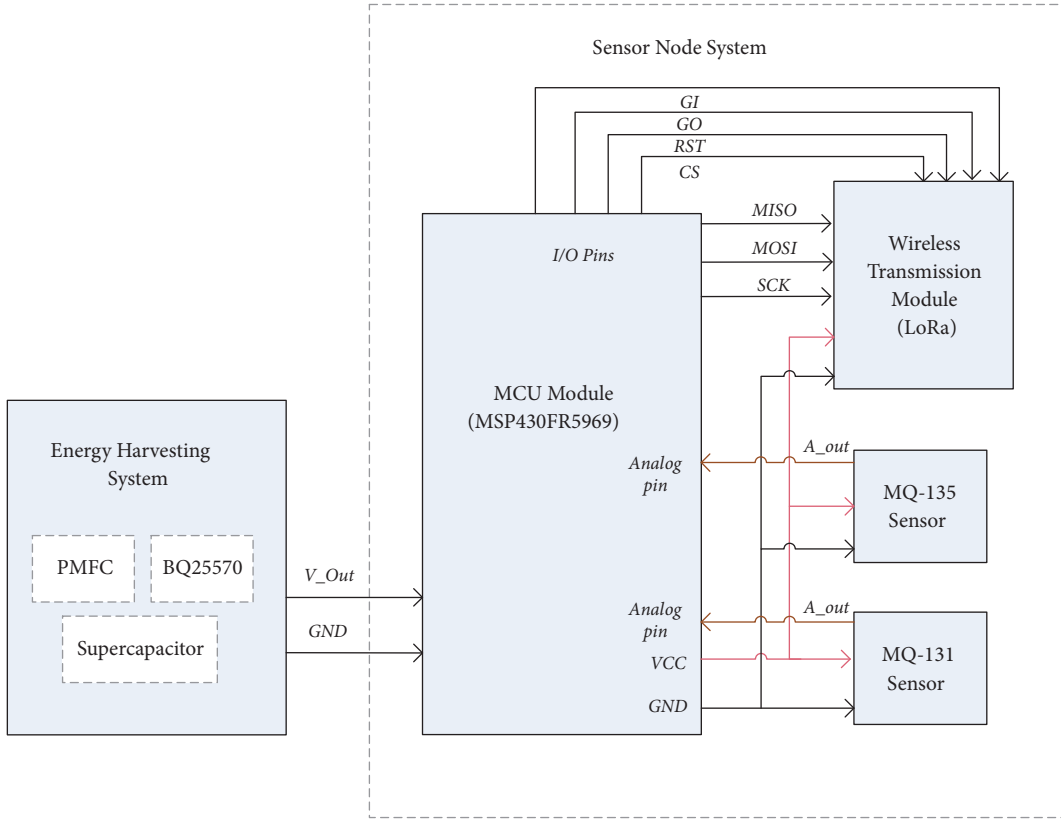

Figure 4: Schematic diagram of the sensor node.

sampling network to optimize the transfer of power within the device. Finally, the BQ25570 was designed with the flexibility to support a variety of energy storage elements.

2.3. Sensor Node Design. The sensor node is composed of three components: microcontroller, sensors, and LoRa transceiver radio. Figure 4 illustrates the schematic circuit of the sensor node. The characteristics of the components are described in the following subsections.

2.3.1. Sensor Module. The data acquisition of the ozone and carbon dioxide is performed using the MQ-131 and MQ-135

sensors, respectively [27], [28]. The main features of the sensors are fast response, high sensitivity, and wide detecting range and do not need a complex drive circuit. Both sensors are composed by a micro AL_2O_3 ceramic tube, a sensitive layer, measuring electrode, and heater fixed into a crust. Standard condition operation is power and heating voltages of 5V ±0.1, the heater resistance is 33 Ω ± 5%, and sensing resistance is 50 kΩ – 500 kΩ. Also, detection range for CO_2 is 10 ppm – 1000 ppm and 10 ppb to 2000 ppb for O_3 gas.

2.3.2. Digital Signal Processing Module. The MSP430FR5969 is an ultra-low power microcontroller unit (MCU) from Texas Instruments with up to 64 KB of non-volatile Ferroelectric Random Access Memory (FRAM). The MCU also supports optimized ultra-low power modes, such as standby (LPM3) and real-time clock (LPM3.5) with a typically power consumption of 0.4 μA and 0.25 μA, respectively. Moreover, its architecture consists of a 16-bit RISC with up to 16 MHz clock supporting a supply voltage range from 1.8 V to 3.6 V [29]. The Code Composer Studio IDE with EnergyTrace™ tool is used to measure and display the energy consumption of MCU and peripherals.

2.3.3. Wireless Transmission Module. The LoRa transceiver device is the RFM95W, which operates in 868.1 MHz unlicensed band and it is based on the SX1276 LoRa module with SPI interface. This radio can transmit as far as 2 km in line of sight or up to 20 km with directional antennas according to the standard. The output power can be tuned in software from +5 to +20 dBm, with a ~100 mA peak current within maximum power output and ~30 mA during active radio listening [19]. Also, an OMNI-directional and 5 dBi gain antenna is coupled to the radio transceiver. In addition, LoRaWAN-Class A is used as a Medium Access Control (MAC) protocol. The Class A MAC protocol opens a transmission window followed by two downlink windows allowing a bidirectional communication with the gateway.

2.4. WSN Architecture. The WSN is composed of three elements: (i) the SNs, (ii) the gateway module, and (iii) an IoT SW application to analyze and manage data coming from SNs. The gateway receives the data and upload the information to a cloud server via WiFi. The network topology is the star configuration. Figure 5 shows the SNs deployment on the Chetumal campus of the University of Quintana Roo, Mexico as a proof of concept of a smart city application.

3. Experimental Results and Discussion

In this section, the PMFC-based LoRa sensor network is evaluated. An experiment with the PMFC, SN, network topology, and power management strategy is presented.

3.1. PMFC. The experiment setup is the following: the PMFC consists of a Sansevieria asparagaceae plant in a plastic container with a volume of $V = 9500\ \text{cm}^3$ ($h = 30$ cm and $d = 20$ cm), filled with 5 kg of a mixed nutrient-rich soil and 125 gr of industrial fertilizer as a salt bridge. A zinc

Figure 5: PMFC-based LoRa WSN architecture.

(Zn) mesh and copper (Cu) wire were used as anode and cathode, respectively (see Figure 2 for details). The PMFC considers a realistic soil sample gathered in University of Quintana Roo, Mexico. It is important to remark that C3 and C4 types of plants are rich for microbiome proliferation, which means that if the organic matter area (or plant root zone) is increased, it will impact in the generation of electrical energy. Thus, the microbial population at the rhizosphere (roots area over the cathode) acts as a biocatalyst for the uptake of root exudates as a substrate and releases redox equivalents (electrons and protons) during its metabolic activity generating energy as voltage/power [19].

To ensure the presence of the electrochemically active bacteria, a mix of organic matter at 100% humidity with diammonium phosphate industrial fertilizer FERTIQUIM [30] is applied into the PMFC. FERTIQUIM composition is 18% of nitrogen (N), 18% of ammonium (NH_4), 46% of phosphorous pentoxide (P_2O_5), 2.20% of soluble sulfur (S), and PH in solution (level 6-7) at 10%. The electrical performance of PMFC was measured using Metrohm Autolab model potentiostat.

In the experiment, the PMFC was stressed along 30 cycles for one week, in order to observe its polarization curve. Figure 6(a) illustrates the polarization and power density curves showing that PMFC voltage is inversely proportional to the output current; also Figure 6(b) shows a voltage and current ranging from 0.8 to 1.25 mW/cm^2 per electrode area that delivers the maximum power density to each cycle. Likewise, it can be seen that a hysteresis effect (i.e., dynamic behavior) is produced and accentuated on the maximum power level, which is related to the initial stabilization of the electron and proton production generated by the bacteria. Figure 6(b) also presents the maximum power density value reached in the polarization curve.

The current density and voltage generated by the PMFC using a load resistance of 1 kΩ considering a constant

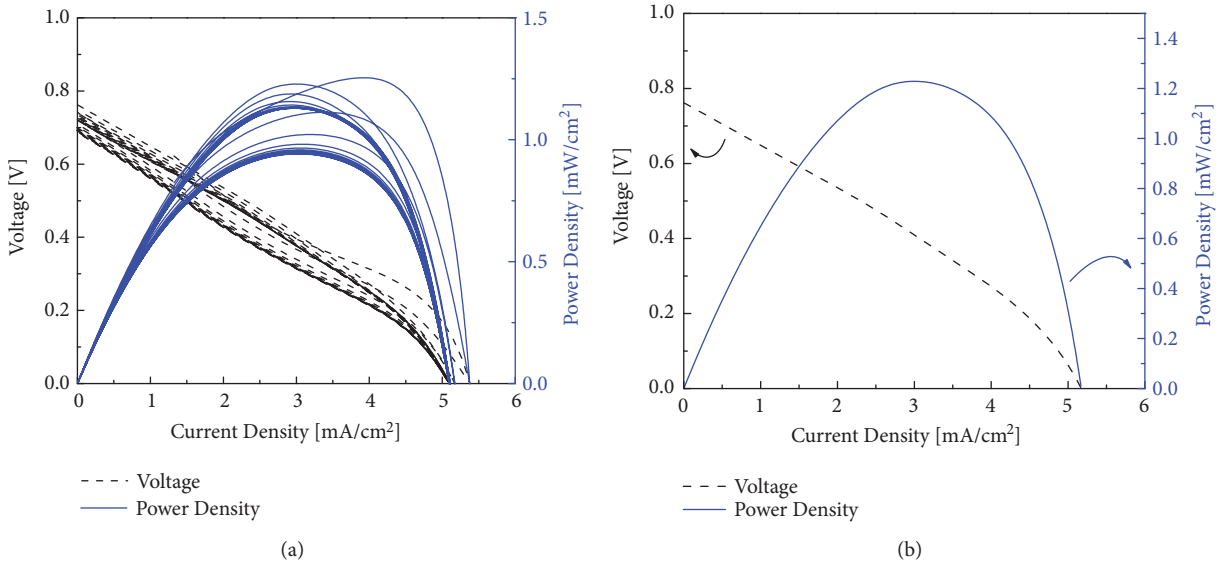

Figure 6: Polarization curve and power density of the designed PMFC. (a) PMFC behavior for 30 cycles and (b) PMFC behavior for the maximum power density reached (1.25 mW/cm^2).

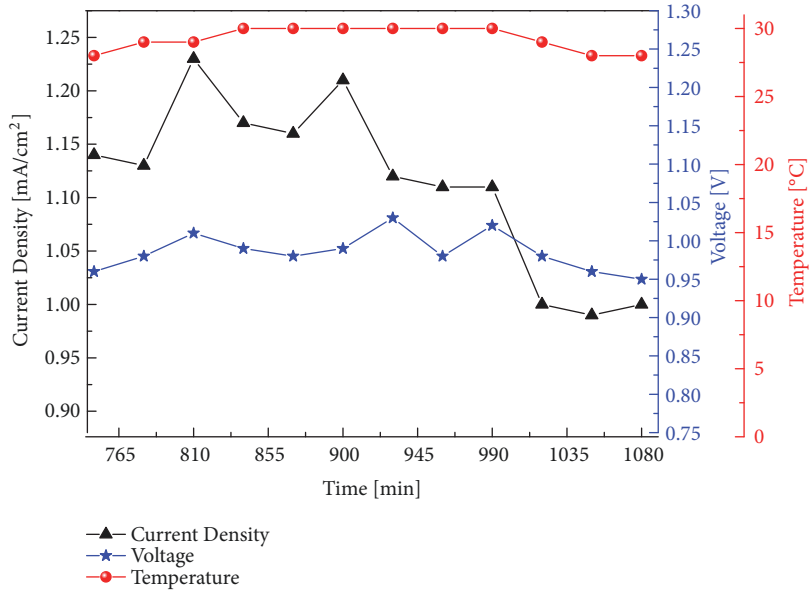

Figure 7: Measured electrical parameters of PMFC versus time.

outdoor temperature of 30°C are shown in Figure 7. The measurements were carried out every 50 min, from 12:00 h to 18:00 h. The average values measured of voltage and current density were 1.00 V and 1.125 mA/cm^2 with a variation of 0.1 V and 0.225 mA/cm^2, respectively, and the maximum current density was produced at 810 minutes (13:50 h).

The stability of the PMFC as power source is one of the main issues in this study. The analysis of the power density for different charging values and its dynamic behavior depend on the number of cycles in time. Figure 8 shows the voltage and power density, when the PMFC provides a constant current of 2.35 mA. Both voltage and power density decreased down to 0.4 V and 1 mW/cm^2 in average, respectively. Also it can be seen that the electrical parameters were recovered after 5 min.

Figure 9 shows another experiment for 45 min, in which the PMFC did not receive water (or fertilizer) along the first 15 min (see the black continuous line in the figure), then the PMFC was irrigated with water. In the experiment, the PMFC was continuously stressed with the Metrolab equipment demanding a constant output voltage of 0.3 V. It can be notice that after the first 15 min the current density of the PMFC was recovered (see the dashed red line in the figure).

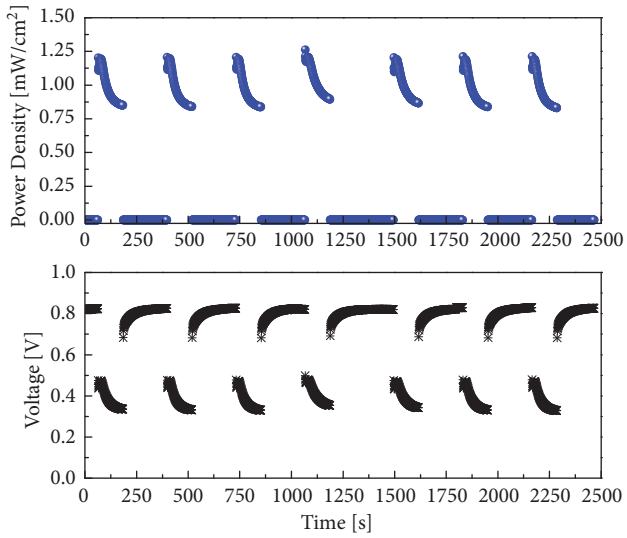

Figure 8: PMFC behavior under discharge and recovery stages of its voltage and power density providing a constant current of 2.35 mA.

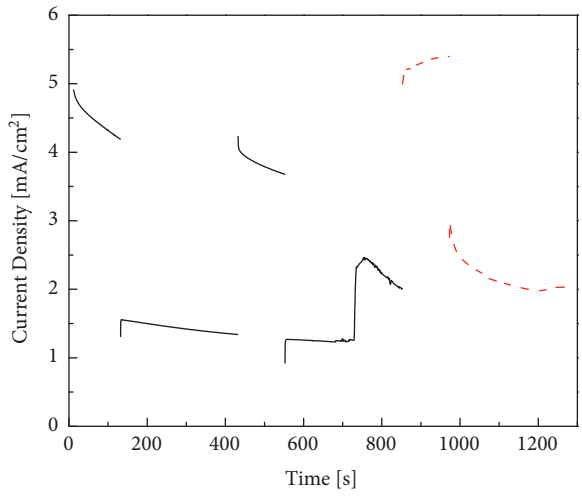

Figure 9: Current density versus time of the PMFC with a recovery stage.

3.2. Energy Harvesting Circuit. The BQ25570 circuit is a nano-power energy harvester solution for ultra-low power application. This power management circuit was connected to an external supercapacitor of 0.1 F to storage the energy. In this process, the boost charger output, V_{Stor}, is configured to deliver up to 4.2 V. This voltage is applied to the supercapacitor as long as V_{BAT} is below to the programmed maximum voltage V_{BAT_OV}. The V_{BAT_OK} indicator toggles high when V_{Stor} increases up to 3.3 V and toggles down when V_{Stor} goes below to 2.8 V.

3.3. Sensor Node Design. The dynamic power management strategy considers five processing stages of the sensor nodes. Figure 10 presents the processing flow diagram of the sensor node. The first stage requires 47 ms and setups the sensor

Table 1: LoRa configuration parameter selection.

SF	Frequency Channel (Mhz)	BW (Mhz)	CR	Transmission Power (dBm)
7	868.1	125	4/5	14

Table 2: Duty cycling schemes.

Transmission intervals (min)	Power (mW) (Max / Mean)	Current (mA) (Max / Mean)
5	166.25 / 3.47	46.36 / 0.96
10	158.98 / 3.09	44.34 / 0.86
20	164.37 / 2.92	45.85 / 0.81

node configuration such as the spreading factor (SF), frequency channel, channel bandwidth (BW), coding rate (CR), and transmission power. In the configuration, short periods of 8 ms are used to achieve the gas concentration. These fast responses in the sensor read measurements are related to stable temperature and humidity environment and to a reduced sensors resistance ratio between the target gas concentration and the resistance of the sensor. The `sense_interval` and `tx_interval` can be adjusted according to the application. In this study, time periods of 5, 10, and 20 min were considered. Both `sense` and `Tx` intervals are configured in LPM3 low-power mode, which means an average power consumption down to 2.92 mW for a time period of 20 min. After the `sense_interval`, the MCU wakes up to read during 8 ms the ozone and carbon dioxide sensors with a bit rate of 12500 bps, then the SN returns to sleep mode and remains a `tx_interval` before the uplink transmission is executed. The transmission stage requires 63 ms, and finally two response windows are opened (i.e., RX1 and RX2 in Figure 10) of 10 ms and 30 ms, respectively, in order to establish bidirectional communication with the application server. Table 1 shows the LoRa radio parameters selection used for the experiment.

Figure 11 shows the real-time behavior of the SN power consumption, and Table 2 summarizes the measured values for different transmission periods. In order to estimate the power and current consumption of the SN, the EnergyTrace software is used for real-time energy-power measurements designed specifically for ultra-low power applications. EnergyTrace technology is included in Code Composed Studio version 6.0 and newer [31]. The resulting maximum and mean power consumption values, with transmission period of 20 min, are equal to 164.37 mW and 2.92 mW, respectively. EnergyTrace software also provides the maximum and mean current consumption of the SN with resulting values of 45.85 mA and 0.81 mA, respectively, for the same transmission interval experiment.

3.4. IoT Monitoring System. A web-server monitoring system was developed for online data visualization and analysis. Figure 12 shows the visual interface of the software application for the measured data in the test field. The interface was implemented using Apache and PHP web design tools. Likewise, in order to comply with security matters, all data is encrypted and transmitted to a cloud platform through a

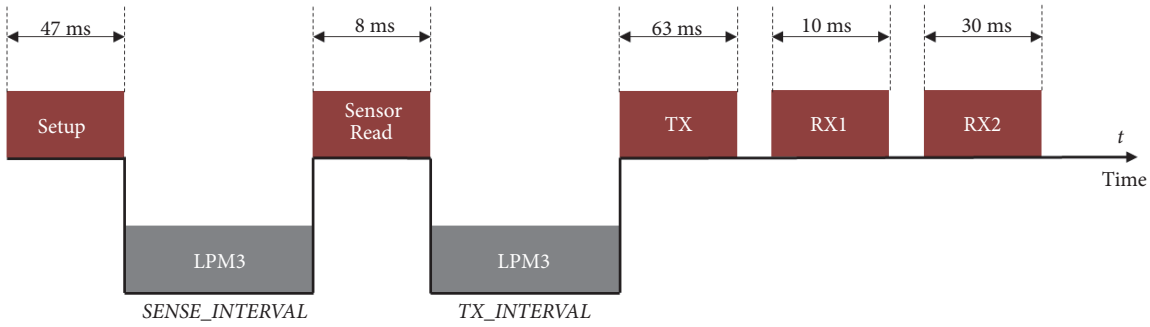

Figure 10: Duty cycle of the sensor node.

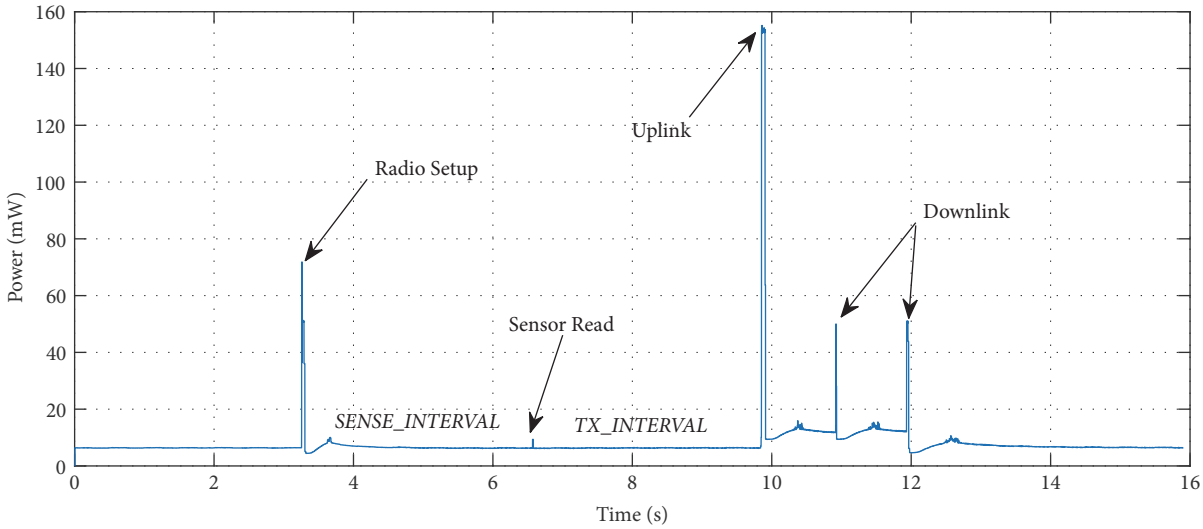

Figure 11: Sensor node power consumption.

(a) (b)

Figure 12: IoT monitoring system for the self-powered PMFC-based LoRa sensor network for environmental analysis in smart cities: (a) sensor node network and (b) visualization of averaged data per day.

LoRa single-channel gateway. The encryption is performed following the activation-by-personalization method defined by the LoRaWAN standard [32]. Also, the sensor data is retrieved from the cloud platform and stored on a local server employing MySQL.

3.5. Discussion. A self-powered IoT system is a power-aware solution for the design of wireless sensor nodes with a batteryless feature. In this sense, the integration of energy conservation and harvesting techniques is demanded for applications in smart cities.

In this study, a PMFC based on the Sansevieria asparagaceae plant is adapted to an energy harvester circuit as a power cell source. PMFC implementation results show that providing a constant current of 2.35 mA to an external device the voltage goes from 0.8 V to 0.5 V. After 2 min, the voltage decreases to 0.33 V, which represents a loss of 42% of the open circuit voltage (0.8 V). Once the load is removed, the

PMFC suddenly recovers 85% of the open circuit voltage and the 100% of its open circuit voltage is recovered after ~4 min. Regarding the power density, it decays to 30% of its initial value (1.25 mW/cm^2) considering the time of discharge and recovery voltage as showed in Figure 8.

In this sense, we can conclude that the PMFC is able to provide a power density of 1.25 mW/cm^2 to the energy harvester BQ25570 circuit, which provides a regulated output of 3.3. V, and stores the energy in a supercapacitor. As illustrated in Figure 11 and Table 2, the mean power consumption of the SN is 3.47, 3.09, and 2.92 mW for transmission intervals of 5, 10, and 20 min, respectively. The test case scenario results reported in Figures 6, 7, 8, 9, and 11 indicate an autonomous operation of the PMFC-based LoRa sensor node.

4. Conclusions

This paper proposes a WSN of self-powered PMFC-based LoRa sensor nodes (SNs) for environmental analysis in smart cities. The system was implemented in the Campus of the University of Quintana Roo in Chetumal, Mexico, as a proof of concept of a smart city, monitoring the surrounding environmental data of ozone (O_3) and carbon dioxide (CO_2) in real time. In the design, a PMFC power cell, based on the Sansevieria asparagaceae plant, was implemented and adapted with an energy harvester circuit to supply a DC output power to the SN. To demonstrate a stable operation, the PMFC was stressed with the Metrohm Autolab potentiostat equipment achieving an adequate performance of 1.25 mW/cm^2 with 0.8 V in open circuit. The used energy harvesting circuit is able to collect the energy from the PMFC regardless of the variations in the charging rates and low input voltages (namely, 100mV). The BQ25570 energy harvester module with nano-power boost charger and buck converter was implemented to manage and store the energy in a supercapacitor. In combination with the PMFC-EH, a dynamic power management strategy was also proposed for ultra-low power consumption of the LoRa-based wireless SN. Experimental results presented in Section 3 showed a SN mean power consumption of 2.92 mW, which is well supported by the proposed PMFC, achieving an autonomous operation of the self-powered PMFC-based LoRa SNs.

Data Availability

The data used to support the findings of this study are available from the corresponding author upon request.

Conflicts of Interest

The authors declare that there are no conflicts of interest regarding the publication of this article.

Acknowledgments

This work was supported by the Programa para el Desarrollo Profesional Docente (PRODEP) 2019, Mexico.

References

[1] A. Zanella, N. Bui, A. P. Castellani, L. Vangelista, and M. Zorzi, "Internet of things for smart cities," *IEEE Internet of Things Journal*, vol. 1, no. 1, pp. 22–32, 2014.

[2] N. A. Pantazis, S. A. Nikolidakis, and D. D. Vergados, "Energy-efficient routing protocols in wireless sensor networks: a survey," *IEEE Communications Surveys & Tutorials*, vol. 15, no. 2, pp. 551–591, 2013.

[3] T. Rault, A. Bouabdallah, and Y. Challal, "Energy efficiency in wireless sensor networks: a top-down survey," *Computer Networks*, vol. 67, pp. 104–122, 2014.

[4] S. Sendra, J. Lloret, M. García, and J. F. Toledo, "Power saving and energy optimization techniques for wireless sensor networks," *Journal of Communications*, vol. 6, no. 6, pp. 439–459, 2011.

[5] F. Engmann, F. A. Katsriku, J.-D. Abdulai, K. S. Adu-Manu, and F. K. Banaseka, "Prolonging the lifetime of wireless sensor networks: a review of current techniques," *Wireless Communications and Mobile Computing*, vol. 2018, Article ID 8035065, 23 pages, 2018.

[6] S. Sudevalayam and P. Kulkarni, "Energy harvesting sensor nodes: survey and implications," *IEEE Communications Surveys & Tutorials*, vol. 13, no. 3, pp. 443–461, 2011.

[7] G. Zhou, L. Huang, W. Li, and Z. Zhu, "Harvesting ambient environmental energy for wireless sensor networks: a survey," *Journal of Sensors*, vol. 2014, Article ID 815467, 20 pages, 2014.

[8] K. Z. Panatik, K. Kamardin, S. A. Shariff et al., "Energy harvesting in wireless sensor networks: a survey," in *Proceedings of the 3rd IEEE International Symposium on Telecommunication Technologies (ISTT)*, pp. 53–58, IEEE, 2016.

[9] X. Lu, P. Wang, D. Niyato, D. I. Kim, and Z. Han, "Wireless networks with RF energy harvesting: a contemporary survey," *IEEE Communications Surveys & Tutorials*, vol. 17, no. 2, pp. 757–789, 2015.

[10] H. Deng, Z. Chen, and F. Zhao, "Energy from plants and microorganisms: progress in plant-microbial fuel cells," *ChemSusChem*, vol. 5, no. 6, pp. 1006–1011, 2012.

[11] D. Brunelli, P. Tosato, and M. Rossi, "Flora health wireless monitoring with plant-microbial fuel cell," *Procedia Engineering*, vol. 168, pp. 1646–1650, 2016.

[12] A. Pietrelli, A. Micangeli, V. Ferrara, and A. Raffi, "Wireless sensor network powered by a terrestrial microbial fuel cell as a sustainable land monitoring energy system," *Sustainability*, vol. 6, no. 10, pp. 7263–7275, 2014.

[13] F. Wu, J. Redouté, M. R. Yuce, and J. Redouté, "WE-Safe: a self-powered wearable iot sensor network for safety applications based on LoRa," *IEEE Access*, vol. 6, no. 40, pp. 846–853, 2018.

[14] E. Osorio de la Rosa, J. Vázquez Castillo, M. Carmona Campos et al., "Plant microbial fuel cells–based energy harvester system for self-powered IoT applications," *Sensors*, vol. 19, no. 6, p. 1378, 2019.

[15] K. Mekki, E. Bajic, F. Chaxel, and F. Meyer, "A comparative study of LPWAN technologies for large-scale IoT deployment," *ICT Express*, 2018.

[16] N. Habibul, Y. Hu, Y.-K. Wang, W. Chen, H.-Q. Yu, and G.-P. Sheng, "Bioelectrochemical chromium(VI) removal in plant-microbial fuel cells," *Environmental Science & Technology*, vol. 50, no. 7, pp. 3882–3889, 2016.

[17] R. Nitisoravut and R. Regmi, "Plant microbial fuel cells: a promising biosystems engineering," *Renewable & Sustainable Energy Reviews*, vol. 76, pp. 81–89, 2017.

[18] N. Tapia, C. Rojas, C. Bonilla, and I. Vargas, "A new method for sensing soil water content in green roofs using plant microbial fuel cells," *Sensors*, vol. 18, no. 2, p. 71, 2018.

[19] P. Chiranjeevi, D. K. Yeruva, K. A. Kumar, V. S. Mohan, and S. Varjani, "Plant-microbial fuel cells technology," *Microbial Electrochemical Technology*, pp. 549–561, 2019.

[20] S. Enríquez, C. M. Duarte, and K. Sand-Jensen, "Patterns in decomposition rates among photosynthetic organisms: the importance of detritus C:N:P content," *Oecologia*, vol. 94, no. 4, pp. 457–471, 1993.

[21] L. Moulin, A. Munive, B. Dreyfus, and C. Boivin-Masson, "Nodulation of legumes by members of the β-subclass of Proteobacteria," *Nature*, vol. 411, no. 6840, pp. 948–950, 2001.

[22] R. Regmi, R. Nitisoravut, and J. Ketchaimongkol, "A decade of plant-assisted microbial fuel cells: looking back and moving forward," *Biofuels*, vol. 9, no. 5, pp. 605–612, 2018.

[23] K. Wetser, E. Sudirjo, C. J. N. Buisman, and D. P. B. T. B. Strik, "Electricity generation by a plant microbial fuel cell with an integrated oxygen reducing biocathode," *Applied Energy*, vol. 137, pp. 151–157, 2015.

[24] M. M. Ghangrekar and V. B. Shinde, "Performance of membrane-less microbial fuel cell treating wastewater and effect of electrode distance and area on electricity production," *Bioresource Technology*, vol. 98, no. 15, pp. 2879–2885, 2007.

[25] S. R. Gilani, A. Yaseen, S. R. A. Zaidi, M. Zahra, and Z. Mahmood, "Photocurrent generation through plant microbial fuel cell by varying electrode materials," *Journal of the Chemical Society of Pakistan*, vol. 38, no. 1, pp. 17–27, 2016.

[26] TI, "Ultra low power management IC, boost charger nanopowered buck converter evaluation module, 2019," http://www.ti.com/tool/BQ25570EVM-206.

[27] Sainsmart, "MQ131 gas sensor ozone module, 2019," https://www.sainsmart.com/.

[28] HiLetgo, "MQ135 air quality sensor hazardous gas detection module, 2019," http://www.hiletgo.com/.

[29] TI, "MSP430FR5969 launchpad development kit, 2019," http://www.ti.com/tool/MSP-EXP430FR5969.

[30] Fertiquim, "Diammonium phosphate, 2019," http://fertiquim.com.mx/wp-content/uploads/2016/06/fosfatodiamonico.pdf.

[31] TI, "Code composer studio (CCS) integrated development environment (IDE), 2019," http://www.ti.com/tool/CCSTUDIO.

[32] N. Sornin, M. Luis, T. Eirich, T. Kramp, and O. Hersent, "LoRaWAN Specification, LoRa Alliance Std, 2016".